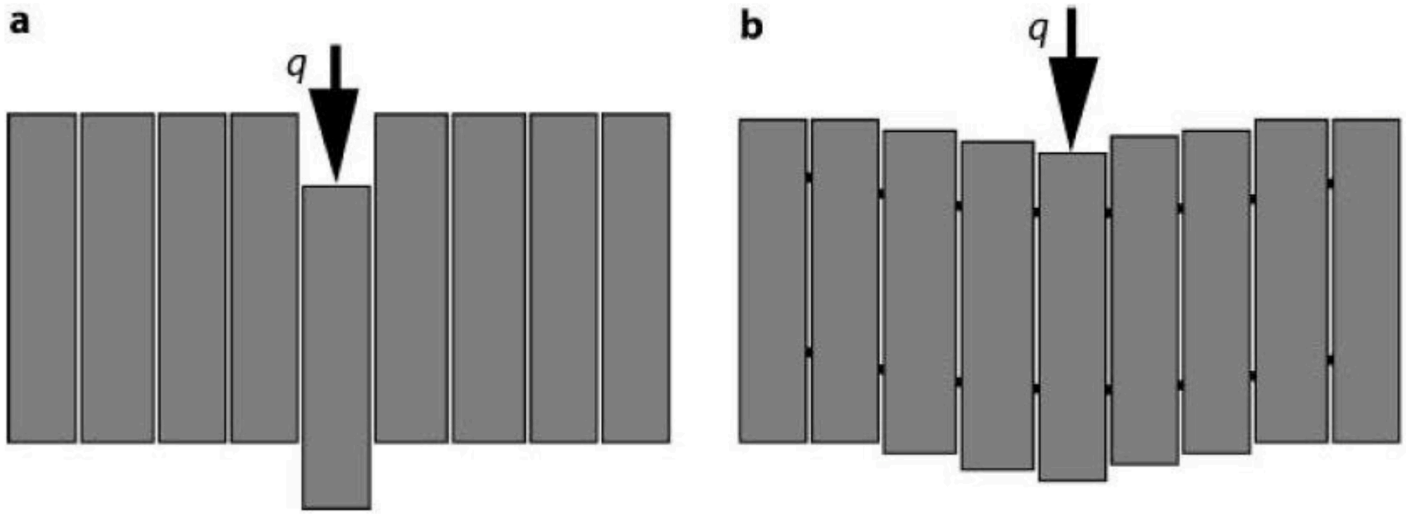

Figure 4.14. Illustration of the difference between **a** hydrostatic isostasy and **b** flexural isostasy. In **a** all vertical columns are considered independently of each other. In **b** the shear stresses between vertical columns are akso considered. q is the load

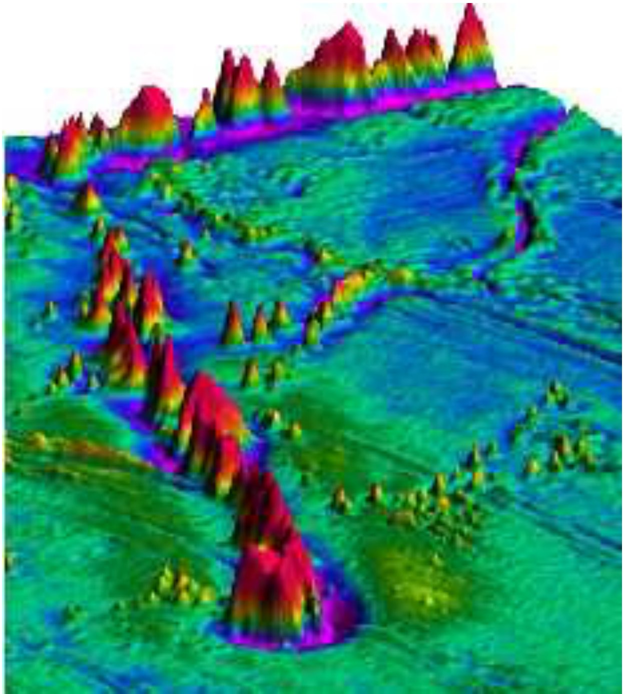

Isostasy and Flexure of the Lithosphere, Watts, 2001

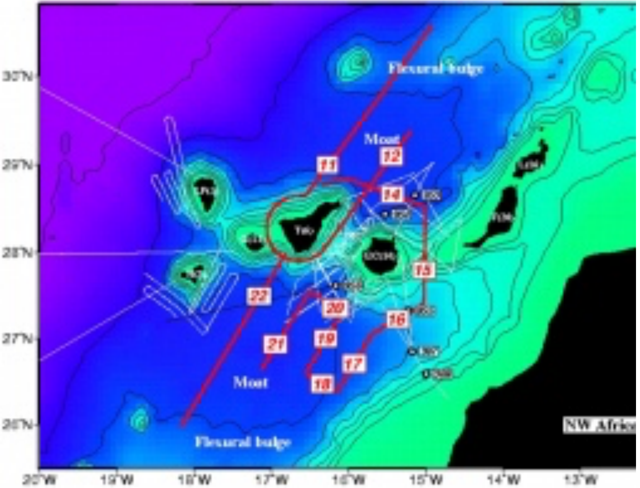

A controlled-source seismic reflection and wide-angle refraction (OBS and landstations) experiment was conducted around the central Canary Islands. The results showed the oceanic basement to be flexed downwards beneath the volcanic loads, forming a moat infilled by 2-3 km of sediments. This flexure, which has been verified by gravity modelling, can be explained by a model in which Tenerife and adjacent islands have loaded a lithosphere with a long-term (> 106 yr) elastic thickness of approximately 20 km. No significant volume of volcanically underplated material was detected beneath the crust of Tenerife.

Best-fit p-wave velocity model along the Canary Islands transect (centred on the island of Tenerife). Bold solid lines show region of the Moho well constrained by modelled PmP arrivals. Bold dashed lines show interpolated discontinuities which are not constrained by the seismic data. Light dashed lines show velocity contours annotated in km/s. M = Moho. B = oceanic basement (From Watts et al., 1997)

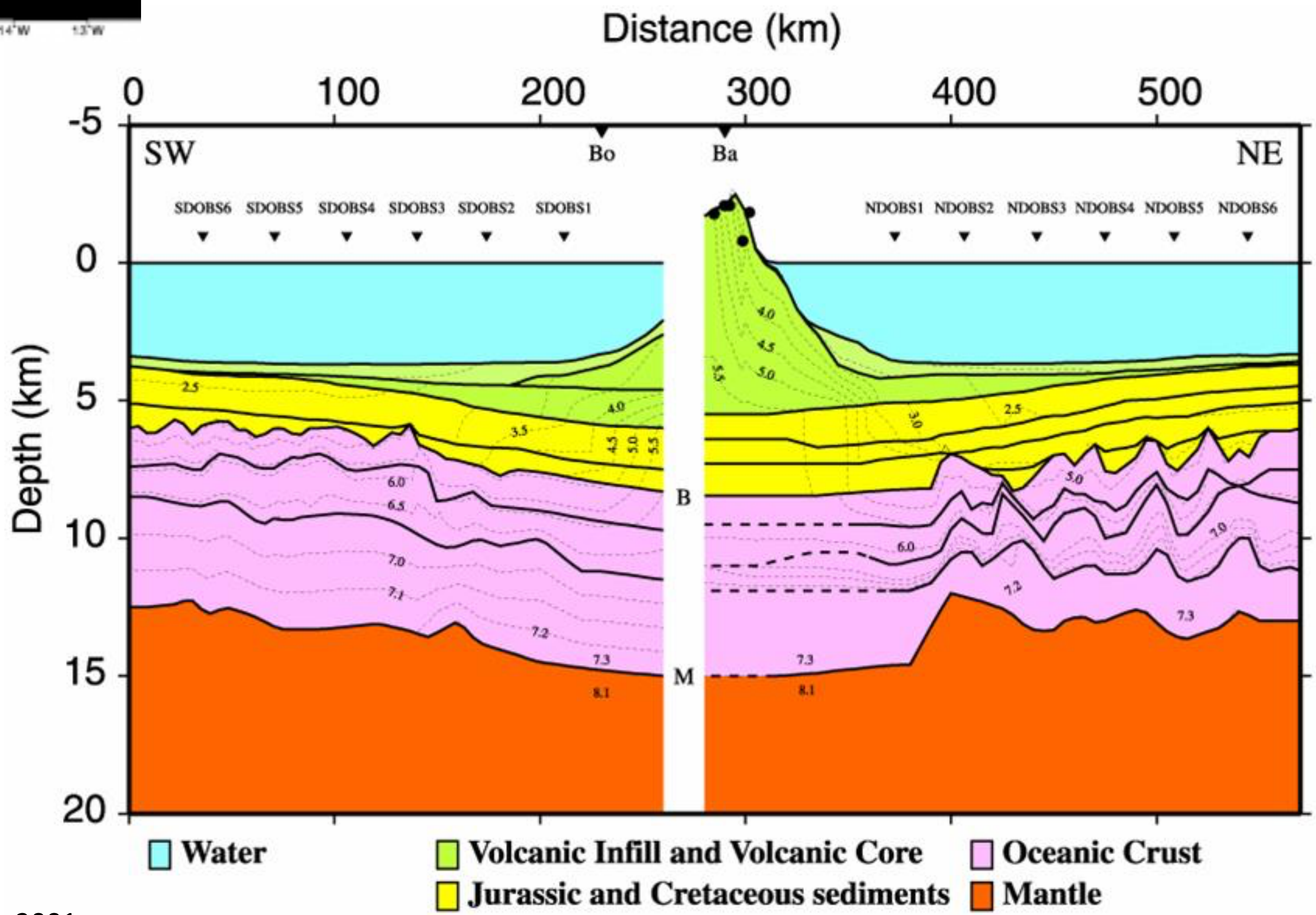

Watts et al., 1997; Collier and Watts, 2001

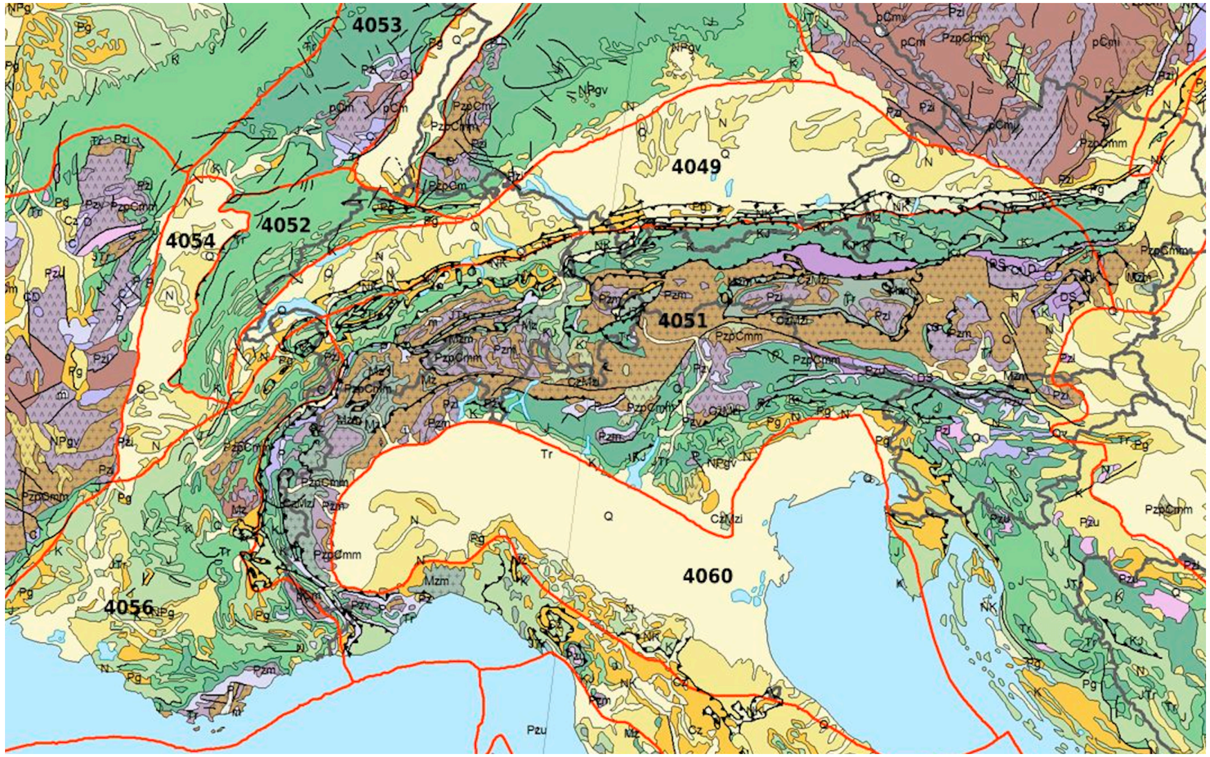

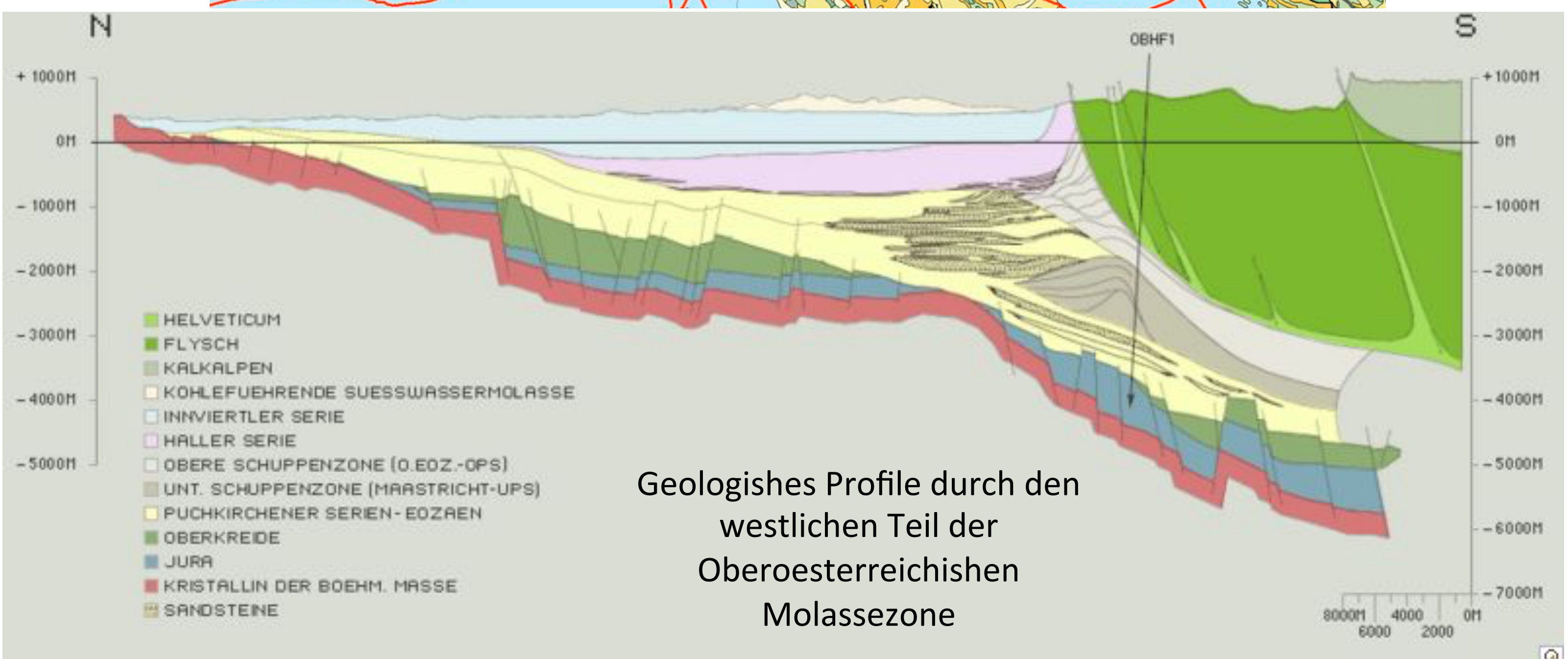

Geologishes Profile durch den westlichen Teil der Oberoesterreichishen Molassezone

East Coast, USA margin

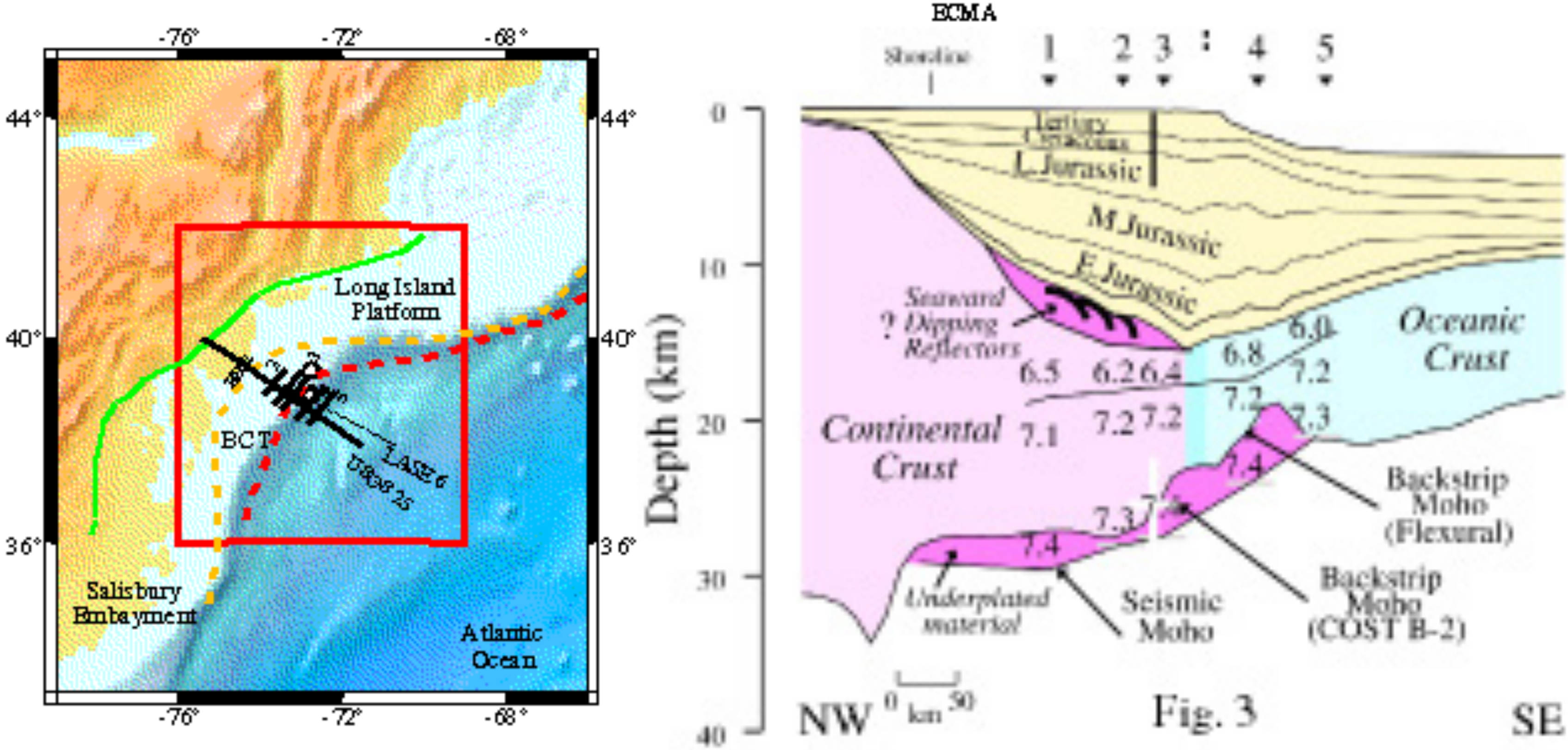

passive pargin, denudational unloading + sediment loading

Deep structure of the US East Coast passive margin from large aperture seismic experiments (LASE), 1986.
Watts, 1988.

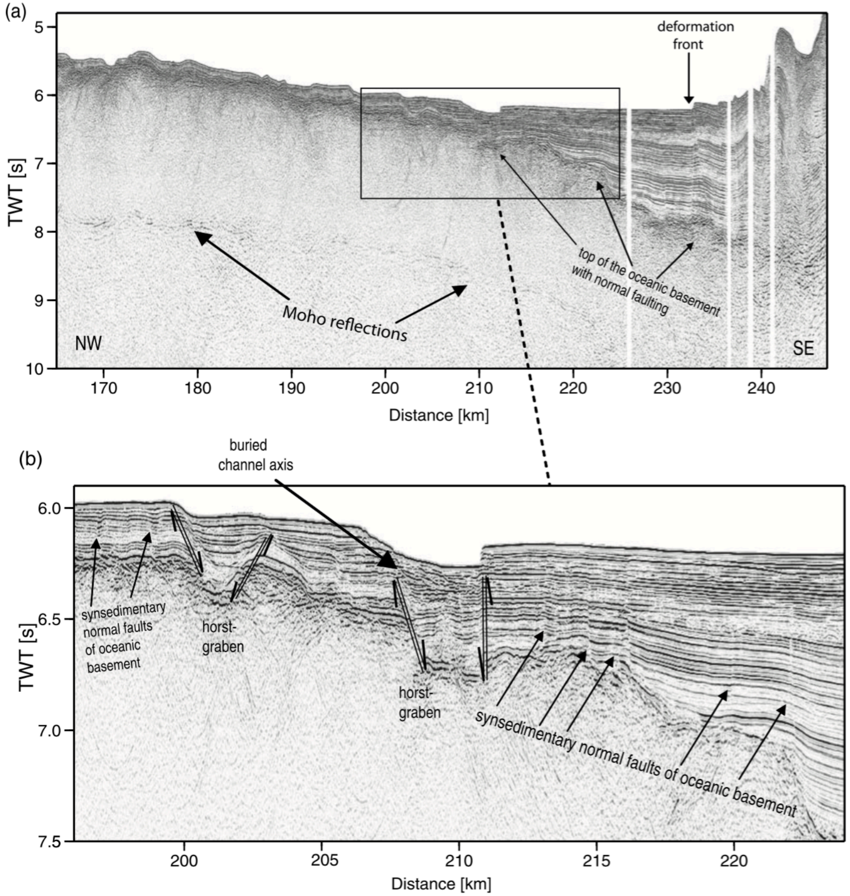

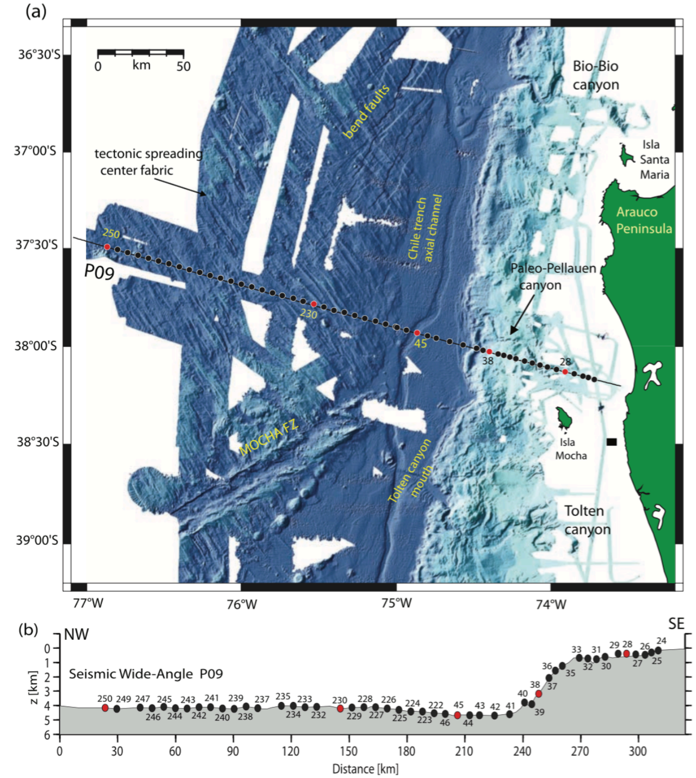

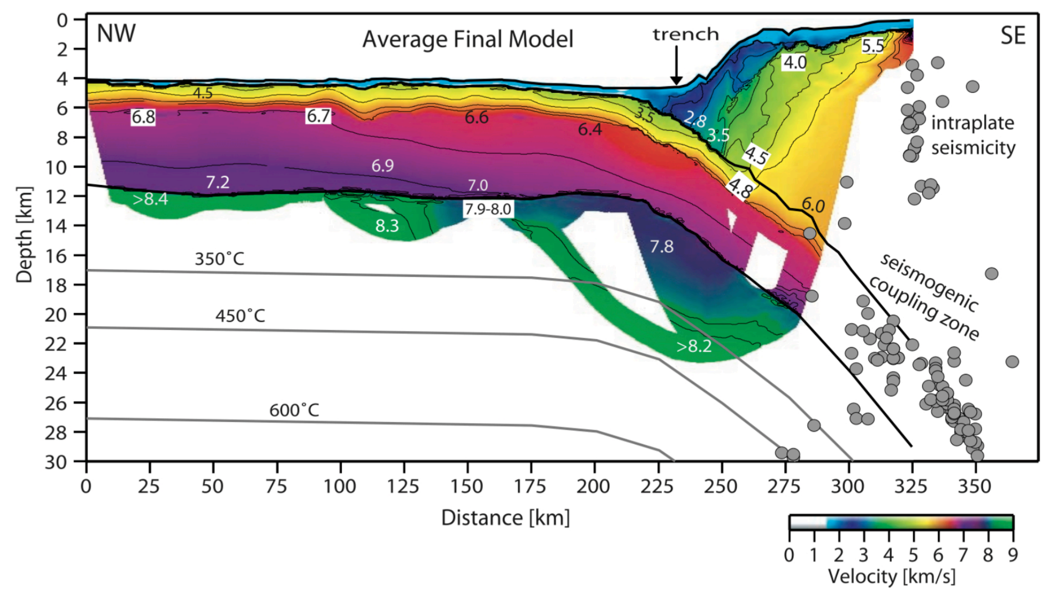

A joint interpretation of swath bathymetric, seismic refraction, wide-angle reflection, and multichannel seismic data was used to derive a detailed tomographic image o the Nazca–South America subduction zone system offshore southern Arauco peninsula, Chile. […] In the trench–outer rise area, the top of incoming oceanic plate is pervasively fractured and likely hydrated as shown by extensional faults, horst-and-graben structures, and a reduction of both crustal and mantle velocities. These slow velocities are interpreted in terms of extensional bending-related faulting leading to fracturing and hydration in the upper part of the oceanic lithosphere.

Contreras-Reyes et al., 2008

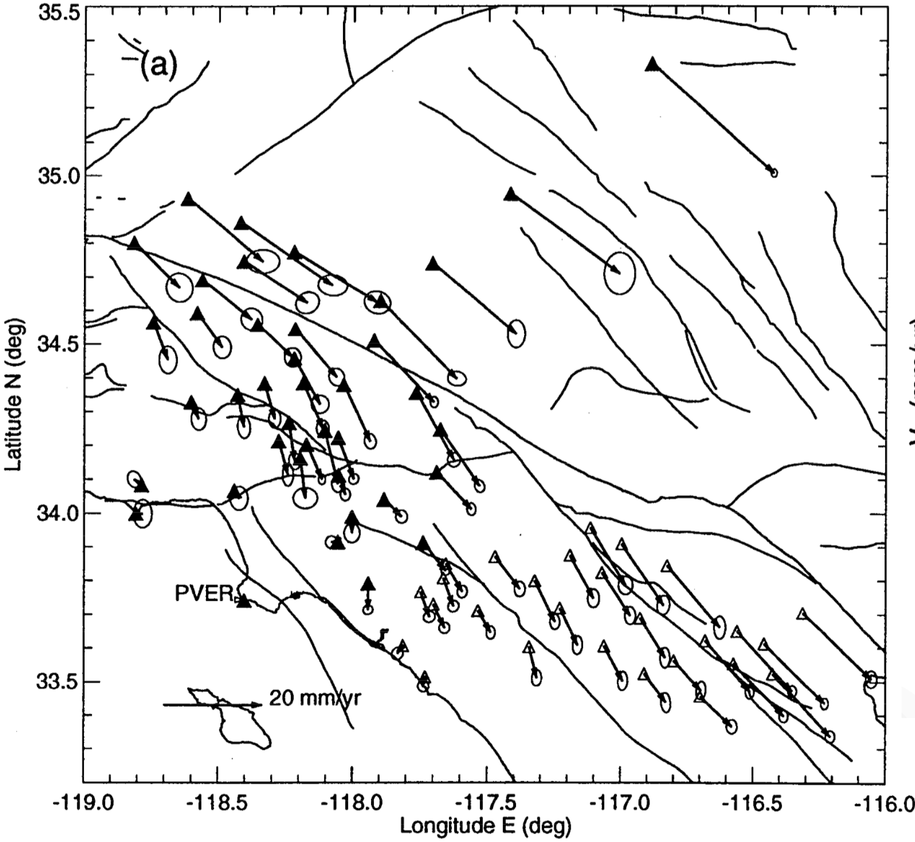

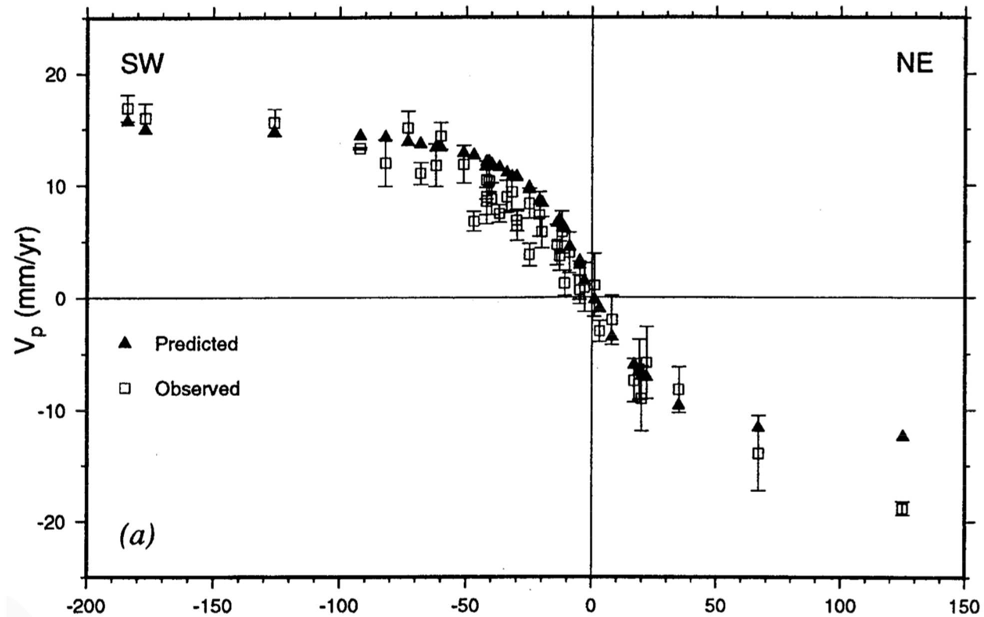

We combine 6 years of Global Positioning System (GPS) data with 20 years of trilateration data and a century of triangulation, taped distance, and astronomic azimuth measurements to derive 66 interseismic station velocities in the greater Los Angeles region.

Shen, Z. K., Jackson, D. D., & Ge, B. X. (1996). Crustal deformation across and beyond the Los Angeles basin from geodetic measurements. *Journal of Geophysical Research*, *101*(B12), 27–957–27–980.

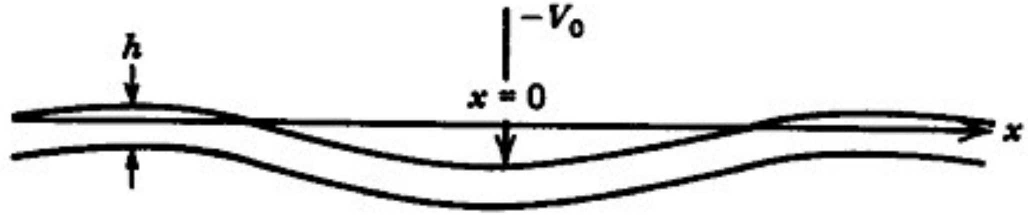

Figure 3-29 Deflection of the elastic lithosphere under a line load.

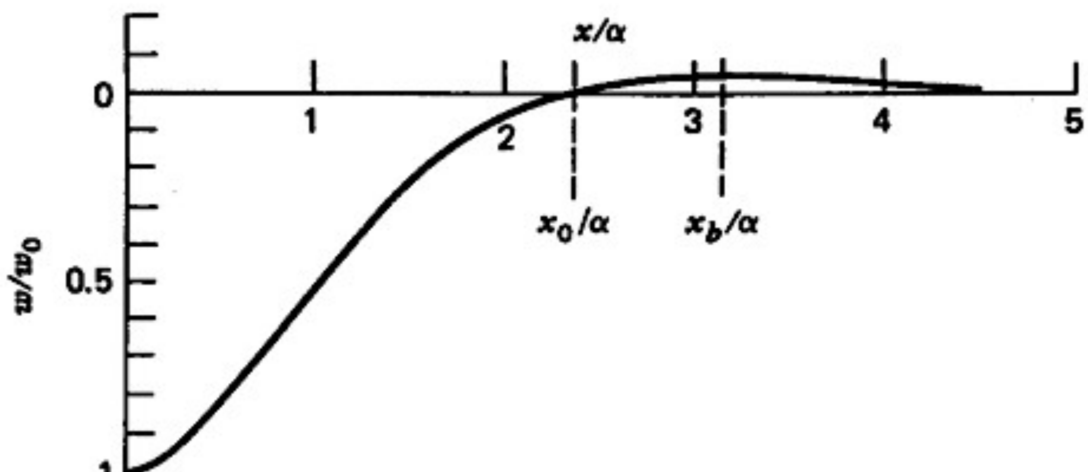

Figure 3-30 Half of the theoretical deflection profile for a floating elastic plate supporting a line load.

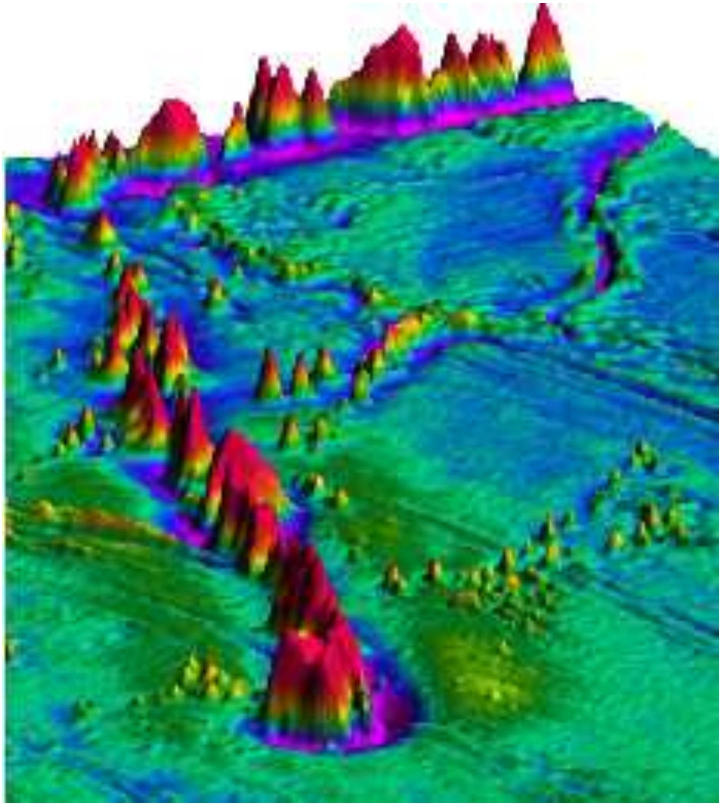

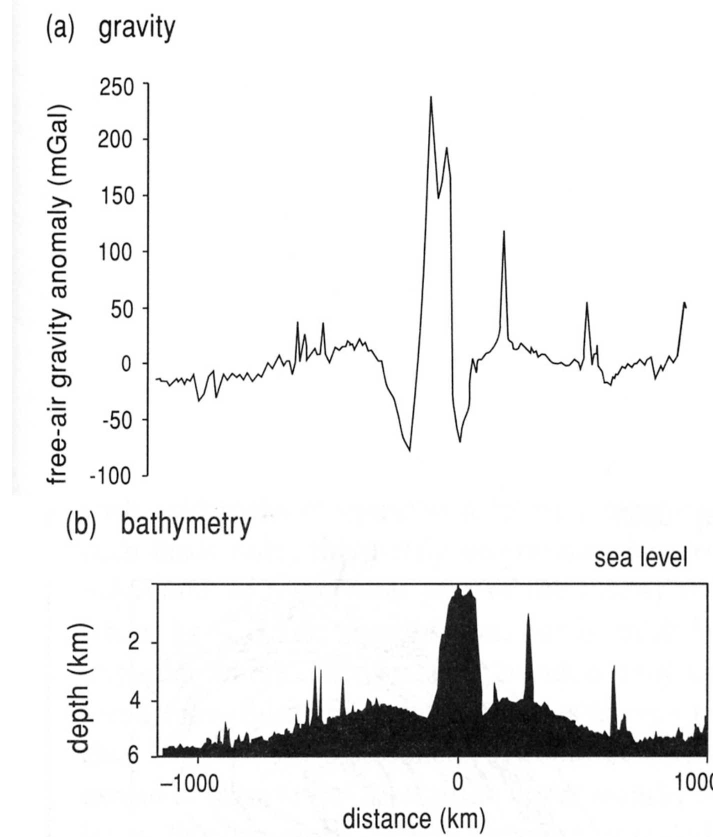

(a) gravity
free-air gravity anomaly (mGal)
250
200
150
100
50
0
-50
-100
(b) bathymetry
sea level
depth (km)
2
4
6
−1000
0
1000
distance (km)

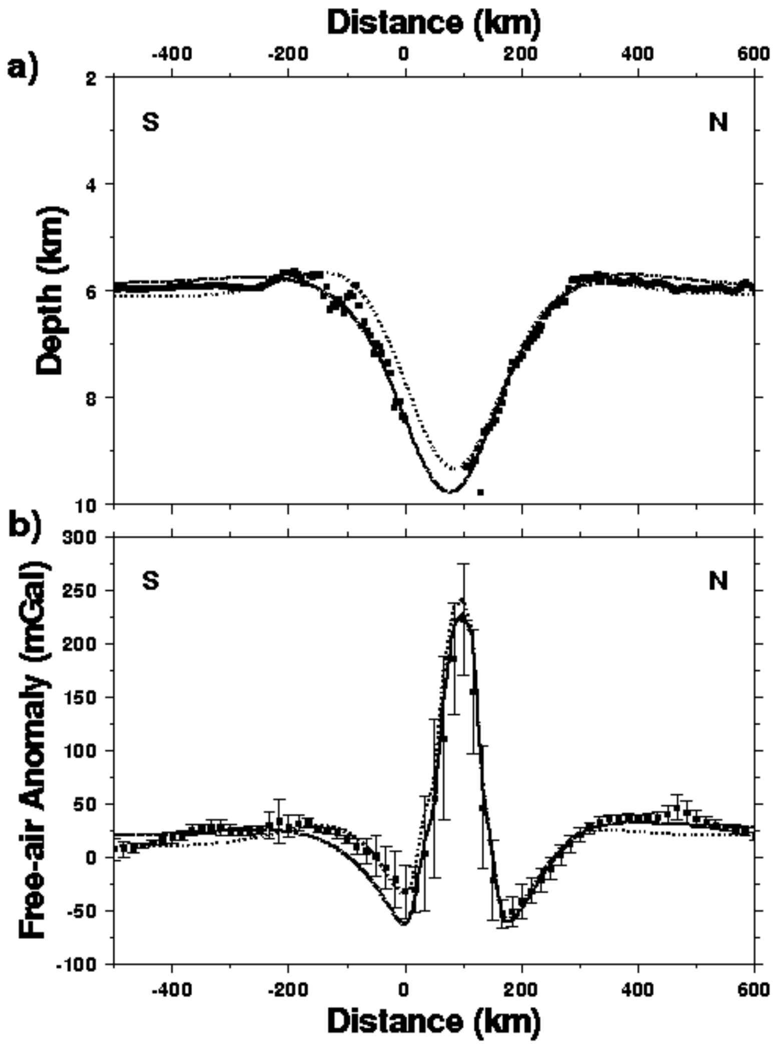

After removal of the very long wavelength (mantle plume) signal:

(a) Best-fitting flexural models using conventional, two-dimensional techniques. The dotted curve is the response of a 25-km-thick elastic plate while the solid curve is the response of a variable thickness plate where the thickness ranges from 35 km away from the load to 25 km beneath the load.

(b) Gravity predictions based on the models in Figure 6a. Within the uncertainties of the data, both models provide reasonable fits, although the constant thickness model fits slightly better

(Wessel et al., 1993).

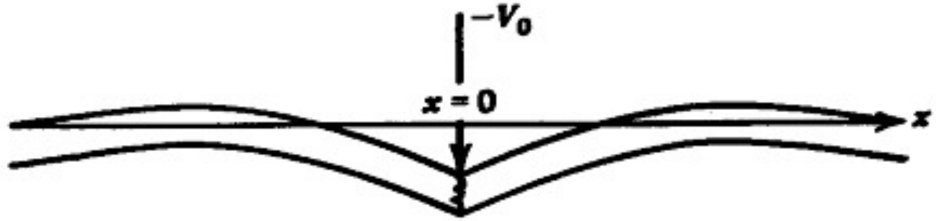

Figure 3-31 Deflection of a broken elastic lithosphere under a line load.

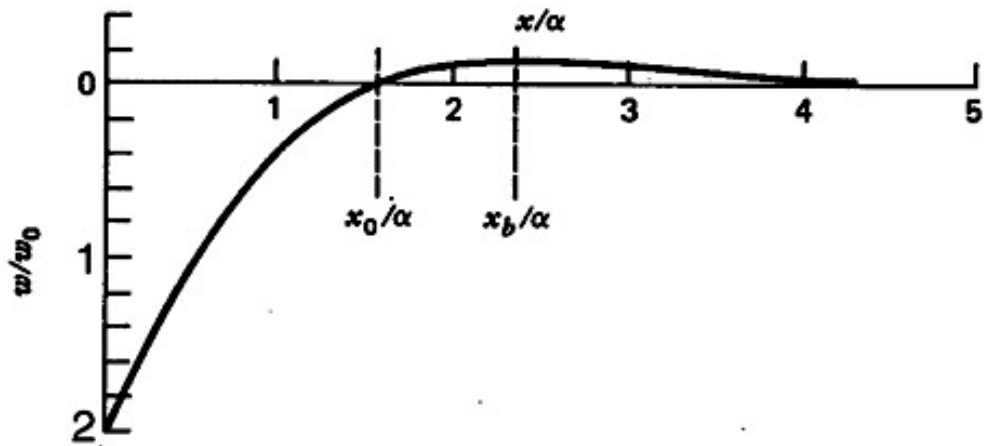

Figure 3-32 The deflection of the elastic lithosphere under an end load.

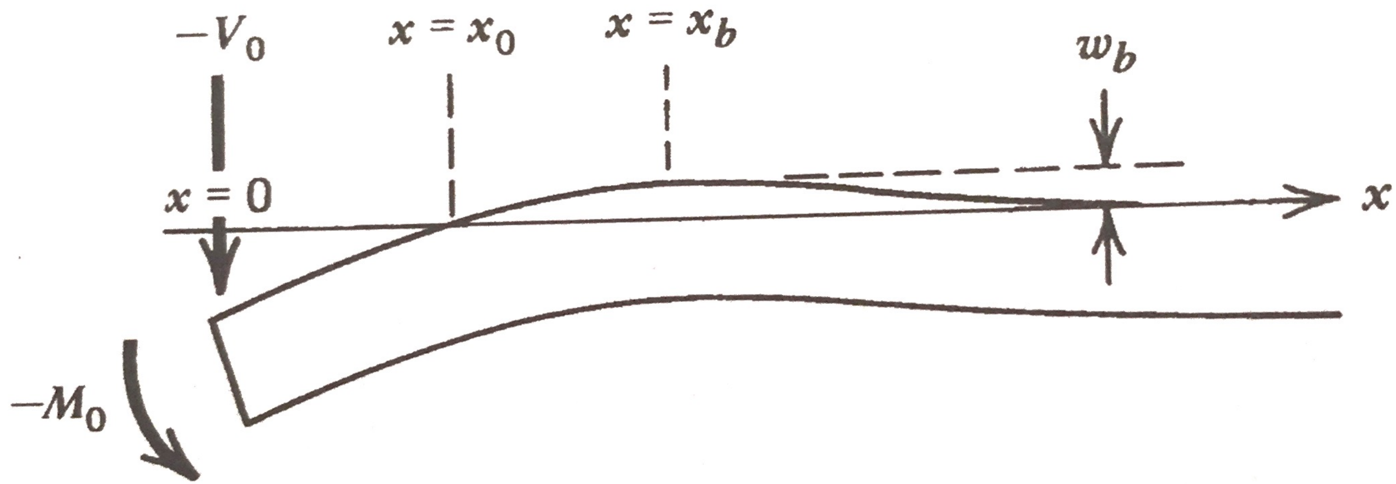

Figure 3.33 Bending of the lithosphere at an ocean trench due to an applied vertical load and bending moment.

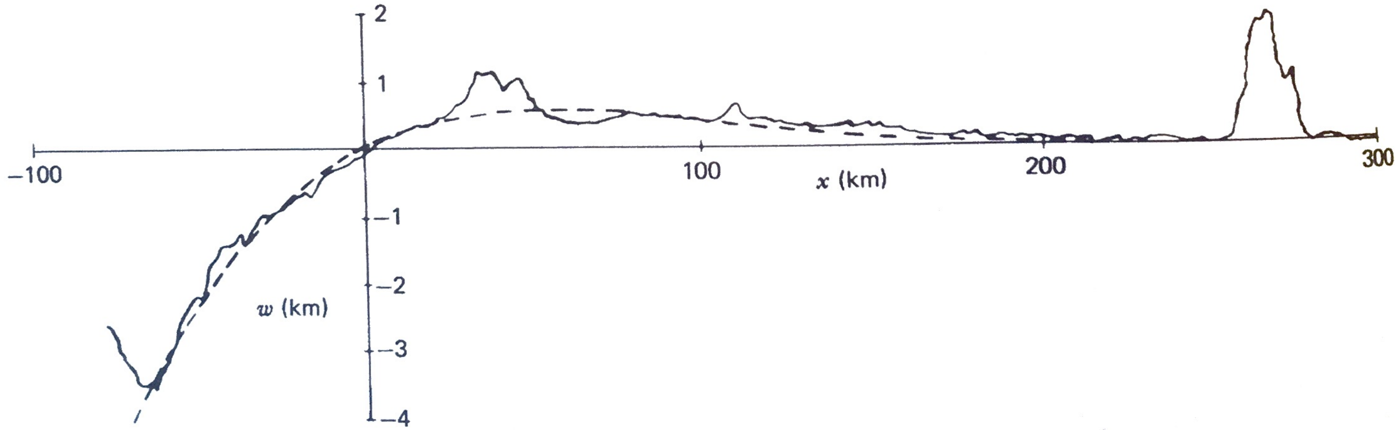

Figure 3.35 Comparison of a bathymetric profile across the Mariana trench (solid line) with the universal lithospheric deflection profile given by Equation (3.159) (dashed line); $x_b = 55$ km and $w_b = 0.5$ km.

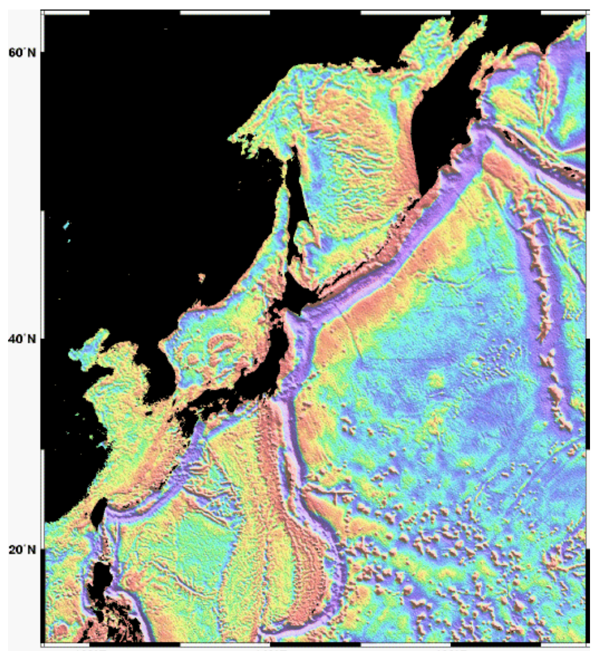

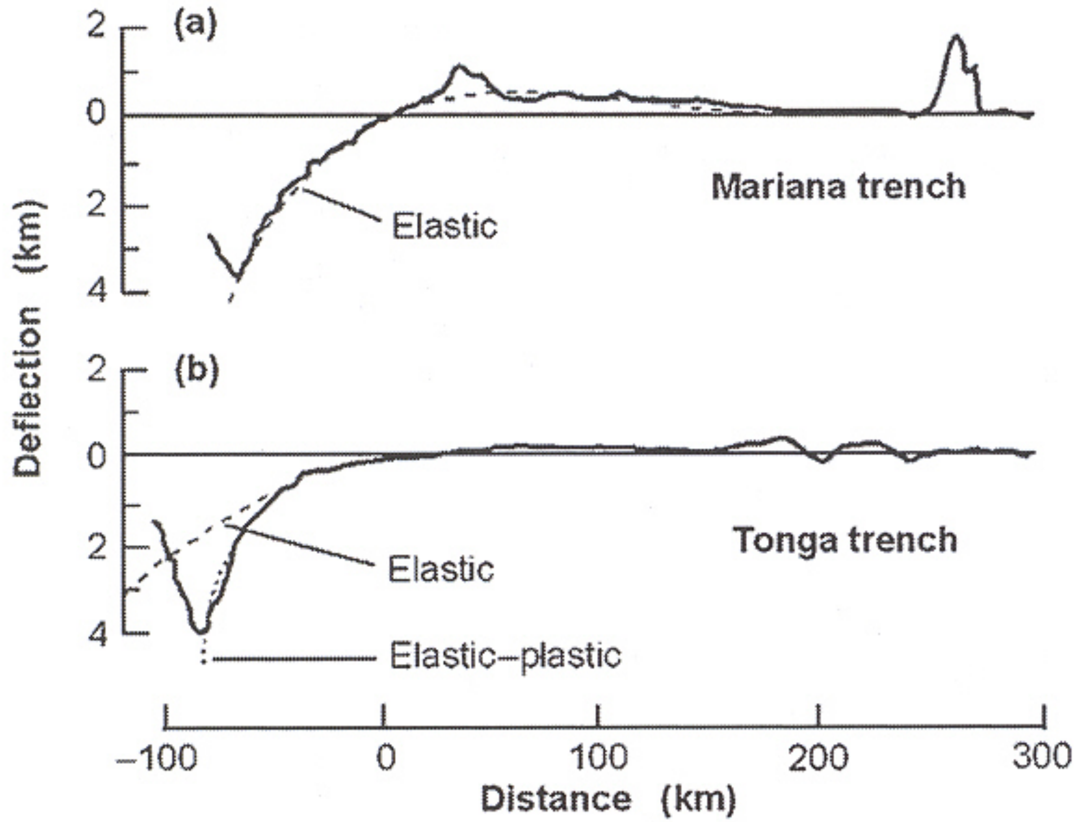

(a)
Mariana trench
Elastic
(b)
Tonga trench
Elastic
Elastic–plastic
Deflection (km)
2
0
2
4
–100
0
100
200
300
Distance (km)

Local compensation (Airy-type here):

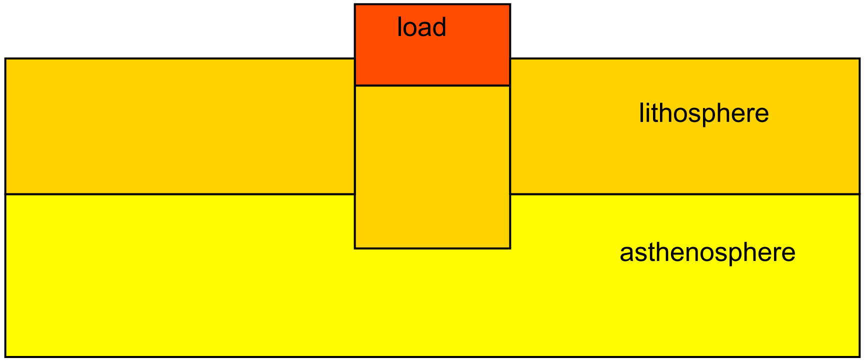

Regional compensation:

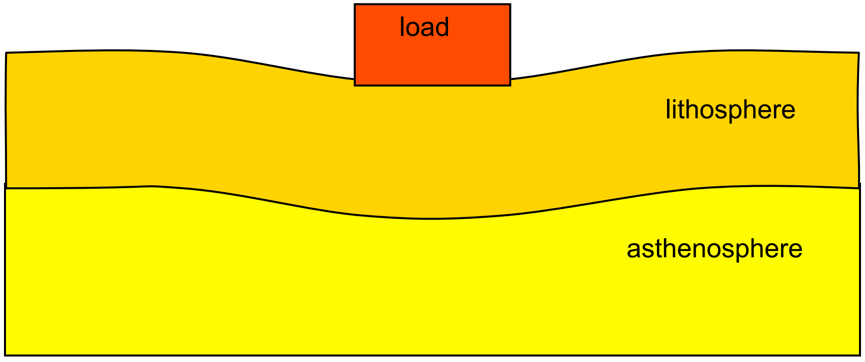

- Deriver GPS elastique! Fait par Romain en sismotectonique en M1